Cluster cross sections from pickup measurements: Are the established methods consistent?

J. Fedor,[a] V. Poterya, A. Pysanenko, and M. Fárník[b]
J. Heyrovský Institute of Physical Chemistry v.v.i., Academy of Sciences of the Czech Republic, Dolejškova 3, 18223 Prague, Czech Republic

Pickup of several molecules, H_2O, HBr, and CH_3OH, and Ar atoms on free Ar_N clusters has been investigated in a molecular beam experiment. The pickup cross sections of the clusters with known mean sizes, $\bar{N} \approx 150$ and 260 were measured by two independent methods: (i) the cluster beam velocity decrease due to the momentum transfer of the picked up molecules to the clusters, and (ii) Poisson distribution of a selected cluster fragment ion as a function of the pickup pressure. In addition, the pickup cross sections were calculated using molecular dynamics and Monte Carlo simulations. The simulations support the results of the velocity measurements. On the other hand, the Poisson distributions yield significantly smaller cross sections, inconsistent with the known Ar_N cluster sizes. These results are discussed in terms of: (i) an incomplete coagulation of guest molecules on the argon clusters when two or more molecules are picked up; and (ii) the fragmentation pattern of the embedded molecules and their clusters upon ionization on the Ar cluster. We conclude that the Poisson distribution method has to be cautiously examined, if conclusions should be drawn about the cluster cross section, or the mean cluster size $\bar{N}$, and the number of picked up molecules.

I. INTRODUCTION

The pickup technique was introduced in mid 1980s for doping clusters with foreign molecules.[1] Since then it has been developed into a very powerful tool in the cluster science: especially numerous experiments with large helium clusters use this technique[2–4] to study the spectroscopy of molecules[5–10] and their reactions[11–15] in the cold superfluid environment of the helium nanodroplets. Here we focus on the pickup to argon clusters which was also exploited in many studies, e.g., for cluster isolated chemical reactions on large Ar clusters in the group of Mestdagh[16,17] and others.[18] The pickup to argon and various other clusters was also employed for studies of photochemistry of molecules in cluster environment,[19–22] and in general for investigation of various mixed molecular clusters.[23,24] Despite these widespread applications of the pickup technique and the earlier studies of this process,[2–4] many questions remain opened concerning the mechanism of the pickup process itself, and sticking, migration and coagulation of the molecules on/in the host clusters – especially for other cluster species than helium nanodroplets. This paper contributes to the detailed understanding of this technique by investigating the pickup process of various molecules (HBr, H_2O, CH_3OH) and argon atoms on large argon clusters.

The second crucial aspect of our paper concerns the pickup cross section and the corresponding cluster size determination. One of the original motivations for cluster studies has been to investigate the evolution of certain properties or processes as a function of the system size.[25] Therefore the cluster size determination has been one of the pivotal issues in the cluster science, which is not a straightforward task for the neutral clusters. Generally, due to the strong fragmentation upon ionization of the weakly bound species, mass spectrometry is of little help here.[26–28] For the small clusters $N \lesssim 10$ the scattering method of Buck and Meyer[26,27] can be exploited to measure the neutral cluster sizes. For the large and medium sizes ($N \sim 10$–10^3) several other methods have been developed, e.g., electron diffraction,[29–32] cluster beam scattering by a buffer gas,[33] pickup of sodium atoms and photoionization,[34] and helium atom diffraction on clusters.[35]

Here we are concerned with two methods for the mean cluster size determination using the pickup process: (1) The first method consists in measuring the variations of the average beam velocity with the pickup pressure.[36] (2) The second one relies on measuring the Poisson distributions of the picked up molecules.[37] Their common feature is that in order to evaluate the cluster mean size $\bar{N}$ from the measured data, the pickup cross section σ has to be determined independently – generally, the geometrical cross section of a hard-sphere was assumed. We assess the two methods by inverting the procedure, i.e., by preparing cluster beam with known mean size $\bar{N}$, evaluating the pickup cross sections σ and comparing them.

We utilized large argon Ar_N clusters with known mean cluster sizes $\bar{N} = 150$ and 260. The argon clusters have been selected as cluster archetypes for several reasons. First, their size distributions were studied in great detail by various methods[35,38–40] and well characterized by Hagena's scaling law.[35,39] Therefore the cluster sizes determined by the

[a] Author to whom correspondence should be addressed. Electronic mail: juraj.fedor@unifr.ch. Present address: Department of Chemistry, University of Fribourg, Chemin du Musée 9, CH-1700 Fribourg, Switzerland.
[b] Author to whom correspondence should be addressed. Electronic mail: michal.farnik@jh-inst.cas.cz.

expansion conditions are well known. Further advantage of Ar_N clusters is, that a fair amount of work exists on the pickup of the present molecules in particular: HBr,[41] H_2O,[37] CH_3OH.[18] This facilitates a critical comparison of the present data obtained by two different methods. Finally, the interaction of Ar-clusters with pickup molecules and atoms can be described by relatively simple potentials and the pickup can be modelled by molecular dynamics and Monte Carlo methods. The theoretically calculated cross sections provide useful references for the assessment of the two experimental methods. Surprisingly the two experimental methods delivered different results. We conclude that the results from velocity measurements are close to the real cross sections while the Poisson distribution method is biased by an incomplete coagulation of the host molecules on the cluster and fragmentation pattern of the host embedded clusters upon the ionization. Also a combination of the two methods is proposed which, in principle, would allow to determine $\bar{N}$ and σ from the experimental data independently without any assumptions of their analytical relation.

II. EXPERIMENT

The principle of the experiment can be briefly summarized as follows: clusters are doped with the guest molecules in a pickup chamber and two characteristics of the cluster beam are measured as a function of the pickup gas pressure – the neutral beam velocity and the fragment ion mass spectra. Our complex cluster beam apparatus was described in detail elsewhere,[42,43] therefore only the parts of the machine relevant for the present experiment are described here and shown in Fig. 1.

The argon clusters were generated in the source chamber S1 by supersonic expansion through a conical nozzle (diameter $d = 50\ \mu$m, length 2 mm, and opening angle $\alpha = 30^\circ$). The nozzle was cooled to a constant temperature of $T_0 = 223$ K and the size of the clusters was controlled by varying the stagnation pressure of argon p_0. The resulting mean cluster size can be determined according to the empirical formulas,[35,39]

$$\bar{N} = K\left(\frac{\Gamma^*}{1000}\right)^{\zeta}, \quad \Gamma^* = \frac{p_0[\text{mbar}]d_e[\mu\text{m}]^{0.85}}{T_0[\text{K}]^{2.2875}}K_c, \tag{1}$$

where $K = 38.4$ and $\zeta = 1.64$ were determined from the diffractive He atom scattering on large Ar_N clusters,[35] $K_c = 1646$ is a characteristic constant of the expanding gas for Ar, and $d_e = \frac{d}{\tan(\alpha/2)}$ is the equivalent nozzle diameter. The applicability of these formulas for rare gas clusters were proved by several experiments,[35,38–40] some of which were done in Göttingen[35] using the cluster source implemented in the present experiments. The two values of stagnation pressure applied in the present experiments $p_0 = 5$ and 7 bars correspond to the mean cluster sizes $\bar{N} = 150$ and 260, respectively.

The Ar cluster beam passed through a skimmer with 1 mm opening before entering the differentially pumped scattering chamber SC. This chamber served as a pickup cell filled with the gas to dope the clusters with molecules. The effective capture length was $L = 17$ cm.[44] The pressure in the chamber was monitored by Bayard-Alpert ionization gauge (Varian type 571), which was calibrated for the specific gases by comparing the measured pressures to the values of a capacitance gauge pressure (Pfeiffer CMR 365). The background pressure in the pickup chamber was $\leq 1 \times 10^{-6}$ mbar, and the pressure with the pickup gas went up to 7×10^{-4} mbar.

For the velocity measurements the cluster beam was modulated by a pseudorandom mechanical chopper[45] (PRC) in the next differentially pumped chopper chamber CC. The chopper contained two pseudorandom sequences of 127 elements and its rotation with frequency of 492.1 Hz corresponded to a single opening time window of 8 μs. After the chopper the beam passed the flight path of 955 mm through the photodissociation chamber PDC (not used in the present experiments) to the ion source of a quadrupole mass spectrometer (QMS) with an electron multiplier detector at the end. The arrival time to the detector was measured. The total flight time was properly corrected for the time spent by the ion fragment in the quadrupole and for any electronic delay of the trigger signals and converted to the beam velocity distribution. The velocity distribution was evaluated from the measured data by the cross-correlation mathematical method.[45] Usually the quadrupole mass spectrometer was set on the major ionization fragment of Ar clusters which is the dimer Ar_2^+ ($m/z = 80$ amu). The maximum velocity of the Ar clusters (without any pickup gas) measured at the nozzle temperature $T_0 = 223$ K was 490 ms^{-1} with a speed-ratio of $S = 35$. This

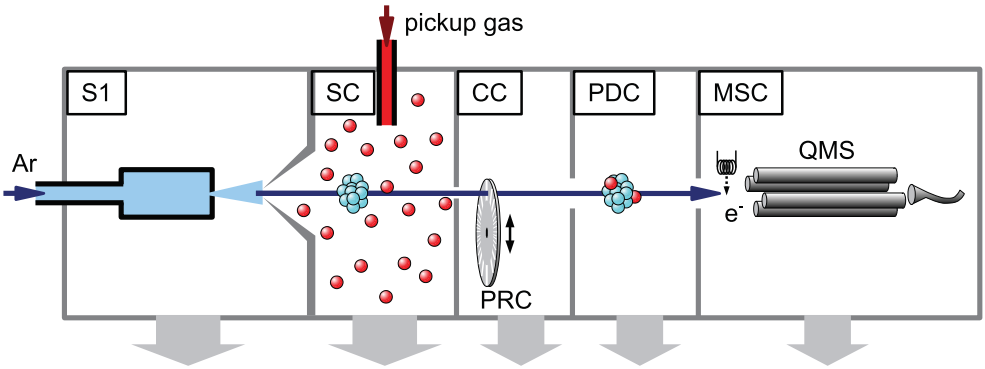

FIG. 1. Schematic picture of the experiment.

corresponds to the theoretical maximum beam velocity,[46]

$$v_\infty = \sqrt{\frac{2k_B T_0}{m}\frac{\gamma}{\gamma - 1}}, \tag{2}$$

where k_B is the Boltzmann constant and γ is the adiabatic index ($\gamma = 5/3$ for a monoatomic ideal gas), i.e., $v_\infty = 481\ \mathrm{ms}^{-1}$. The slightly higher measured beam velocity can be due to the condensation effect which provides an additional heating of the beam during the expansion.

In addition to the beam velocities, the fragment ion mass spectra of the doped clusters were recorded as a function of the pickup gas pressure. The ionizing electron energy was 70 eV. The quadrupole mass spectrometer transmittance was calibrated using the known spectrum of mass calibrant FC-43.

III. PICKUP DYNAMICS AND STATISTICS

Since the argon clusters have a solid-like character,[29,30,32] the molecules do not penetrate the cluster upon the pickup and stay in the outer solvation shell,[47–49] and the clusters in the beam are slowed down by the pickup due to the momentum transfer. The velocity change increases with the number of guest molecules.

Let us assume an Ar_N cluster of a size N with an initial velocity v_i colliding with k stationary molecules in the pickup cell which stick to the cluster. Then the momentum conservation yields for the cluster final velocity v_f the equation,

$$N m_{\mathrm{Ar}} v_i = (N m_{\mathrm{Ar}} + k m_X) v_f, \tag{3}$$

where m_{Ar} is Ar atom mass and m_X is the mass of the guest molecule. It assumes that no considerable evaporation of cluster constituents occurs upon the pickup. This assumption has been justified by the molecular dynamics simulations outlined in Sec. V. The simulations also show that the molecule remains on the cluster if a considerable momentum transfer between the molecule and the cluster occurs. Thus this simple model describes the final velocity dependence sufficiently well (see Sec. V).

The number of picked up molecules along the path-length L in a gas at a pressure p (corresponding to the number density $n_g = p/k_B T$) can be expressed as

$$k = n_g \sigma_e L = \frac{p}{k_B T}\sigma_e L, \tag{4}$$

where σ_e is the pickup cross section. The measured effective cross section σ_e incorporates the velocity-averaging correction factor[46,50,51] into the cross section $\sigma_e = \sigma_0\ F_{a0}(\infty, x)$. Combining Eqs. (3) and (4), the relative change in the cluster velocity is directly proportional to pickup cell pressure,

$$\frac{\Delta V}{V} \equiv \frac{v_i - v_f}{v_f} = \frac{m_X}{N m_{Ar}}\frac{L\sigma_e}{k_B T} p. \tag{5}$$

Thus, from the slope of the relative velocity change dependence on the pressure the pickup cross section σ_e can be evaluated.

Since the pickup of the kth molecule is assumed to be a random process independent of the previous $(k-1)$ events, its probability follows the Poisson distribution:[2]

$$P_k(p) = \frac{1}{k!}(\sigma_e L n_g)^k e^{-\sigma_e L n_g} = \frac{1}{k!}\left(\frac{\sigma_e L}{k_B T} p\right)^k e^{-\frac{\sigma_e L}{k_B T} p}. \tag{6}$$

Thus the pickup cross section σ_e can be obtained by measuring the dependence of a fragment ion intensity (corresponding to, e.g., pickup of $k = 1$ molecule) on the pickup pressure, and fitting this dependence with the corresponding Poisson distribution.[3]

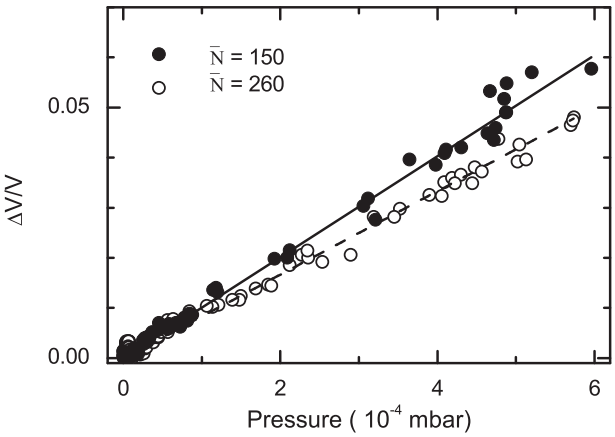

FIG. 2. Relative decrease in the cluster beam velocity as a function of the pickup gas pressure (lines, Eq. (5)) for the pickup of H_2O on Ar_N clusters with $\bar{N} = 150$ and 260.

IV. EXPERIMENTAL RESULTS

A. Velocity measurements

Water H_2O, methanol CH_3OH, hydrogen bromide HBr, and argon Ar were used as pickup gases. According to Eq. (5) the relative change in the cluster beam velocity is directly proportional to the pickup gas pressure. This linear dependence is demonstrated in Fig. 2 for the pickup of H_2O on Ar_N, $\bar{N} = 150$ and 260. The somewhat larger scatter of the data for $\bar{N} = 150$ corresponds to the smaller signals measured for the smaller clusters. Nevertheless, both data sets can be fitted by straight lines with high confidence, in accordance with the previous experiments.[36] Similar dependence was measured for the other pickup species. The pickup cross sections σ_e were derived from the slopes of the linear fits and are summarized in Table I. The error in the velocity measurement is smaller than 1%; however, the uncertainty due to the pressure calibration can be up to 10%.

The quantity that is evaluated directly from the experimental data is the effective cross section,

$$\sigma_e = \sigma_0 \cdot F_{a0}(\infty, x), \tag{7}$$

which incorporates the velocity-averaging correction factor F_{a0} due to the velocity distribution of the target molecules.[46,50,51] Label ∞ denotes the hard sphere potential approximation, and $x = v_i/\alpha_g$ where v_i is the cluster beam velocity and α_g is the most probable velocity

TABLE I. Pickup cross sections for two mean Ar_N cluster sizes $\bar{N} = 150$ and 260 obtained by various methods: velocity measurements, Poisson distribution measurements, and molecular dynamics simulations. The experimental error of σ_e obtained from the velocity measurements was estimated $\lesssim$10%. The Poisson distribution cross section was obtained by fitting the experimental data by $P_1(p)$, Eq. (6), and does not have a real physical meaning as argued in the text. The corrected cross sections σ_0 were evaluated from the experimental σ_e obtained from the velocity measurements divided by the velocity correction factors $F_{a0}(\infty, x)$ (see the text). Correction R_0 to the hard sphere geometrical cross section was evaluated from the simulated cross sections.

		Velocity			Detected ion	Poisson	Simulations	
Molecule	$\bar{N}$	σ_e (Å^2)	F_{a0} (∞, x)	σ_0 (Å^2)	mass (amu)	σ_e (Å^2)	σ_e (Å^2)	R_0 (Å)
HBr	150	672	1.133	593	Br^+ (81)	500	748	4.3
	260	836		738		352	...	
H_2O	150	848	1.545	549	H_2O^+ (18)	528	928	6.1
	260	1083		701		408	...	
CH_3OH	150	1041	1.329	783	CH_3O^+ (31)	561	...	
	260	1523		1146		522	...	
Ar	150	708	1.267	559	...	...	824	5.1
	260	1080		852	...	...	...	

in the Maxwellian distribution of the scattering gas. These correction factors were tabulated in the literature[50,51] and are summarized together with the evaluated σ_0 in Table I.

B. Poisson distributions

Generally the mass spectra of Ar_N clusters doped with the above molecules exhibit three groups of mass peaks: (i) the most pronounced is the sequence of Ar_n^+ peaks; (ii) the ion fragments of the guest molecules and ion fragments of the formed guest clusters; (iii) in some cases there are mixed cluster ions containing Ar-atom(s) and the picked up molecule or its fragment.

When methanol is introduced into the pickup chamber characteristic peaks at $m/z = 31$ amu (CH_2OH^+) and 29 amu (COH^+) appear in the mass spectra. At elevated methanol pressures new peaks raise due to the methanol cluster generation on Ar cluster: 33 amu ($(CH_3OH)H^+$) and 63 amu ($CH_3OH{\cdot}CH_2OH^+$) which can be generated from the methanol dimer and larger clusters $(CH_3OH)_k$, $k \geq 2$; 65 amu ($(CH_3OH)_2H^+$) and 95 amu ($(CH_3OH)_2{\cdot}CH_2OH^+$) which indicate the presence of $k \geq 3$ host clusters; and 97 amu ($(CH_3OH)_3H^+$) fragmenting from $k \geq 4$. There was no evidence for $Ar_n(CH_3OH)_m{}^+$ fragments. Similar spectra were measured for methanol pickup on Ar clusters in other experiments.[18]

From the earlier studies [52–55] of hydrogen bonded clusters, it was found that a fast proton transfer reaction follows the cluster ionization. Thus the major ionization channel results in the protonated fragments with the abstraction of one or more monomer units. The ions below the monomer mass are usually expected to originate from the ionization of a single molecule on the cluster. The intensities of the following ion peaks were plotted against the pressure in the pickup chamber and analysed with the Poisson statistics, see Fig. 3: COH^+ and CH_2OH^+ monitoring the pickup of $k = 1$ molecule; $(CH_3OH)H^+$ and $(CH_3OH)CH_2OH^+$ monitoring $k = 2$ pickup, and $(CH_3OH)_2H^+$ for $k = 3$. This assumes the coagulation of molecules upon pickup on the cluster and the following fragmentation upon ionization:

$$CH_3OH \rightarrow COH^+, CH_2OH^+,$$
$$(CH_3OH)_2 \rightarrow (CH_3OH)H^+, (CH_3OH)CH_2OH^+,$$
$$(CH_3OH)_3 \rightarrow (CH_3OH)_2H^+,$$

i.e., no population of these fragments from larger clusters. We argue in the discussion that our data indicate that these assumptions are not fulfilled completely.

The capture of water molecules results in the observation of peaks at $m/z = 18$ amu (H_2O^+) and 58 amu ($Ar{\cdot}H_2O^+$) presumably from the monomer; 19 amu (H_3O^+) and 59 amu ($Ar{\cdot}H_3O^+$) which can originate from $k \geq 2$; and 55 amu ($(H_2O)_3H^+$) from $k \geq 4$ (the fragment $(H_2O)_2H^+$ at 37 amu indicative of $k \geq 3$ was obscured by the nearby strong Ar^+ peak at 40 amu). It is interesting to note that here, unlike in the methanol case, the ion fragments containing Ar are observed. Again we measure the pickup pressure dependence of

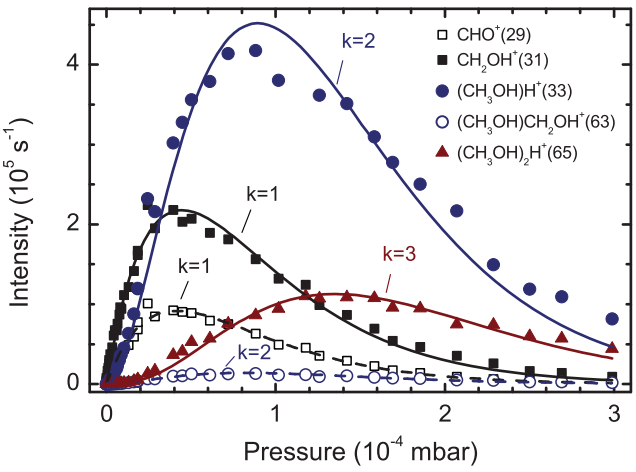

FIG. 3. Intensity of fragment ion peaks in the mass spectra as a function of pickup pressure of CH_3OH. The lines correspond to the Poisson fits P_k, Eq. (6). Detected ions (mass in amu): COH^+ (29) and CH_3OH^+ (31) fitted with $k = 1$; $(CH_3OH)H^+$ (33) and $(CH_3OH)CH_2OH^+$ (63) fitted with $k = 2$; and $(CH_3OH)_2H^+$ (65) fitted with $k = 3$.

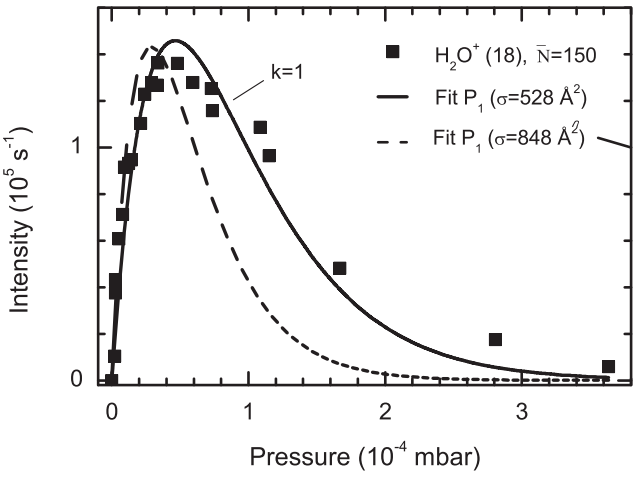

FIG. 4. Intensity of monomer fragment ion peak ($m/z = 18$ amu) in the mass spectrum as a function of water pressure in the pickup chamber. Solid line represents the Poisson distribution fit (Eq. (6)) with $k = 1$ and σ_e as a fitting parameter ($\Rightarrow \sigma_e = 528$ Å^2). The dashed line corresponds to the Poisson distribution with $\sigma_e = 848$ Å^2 obtained from the velocity measurement.

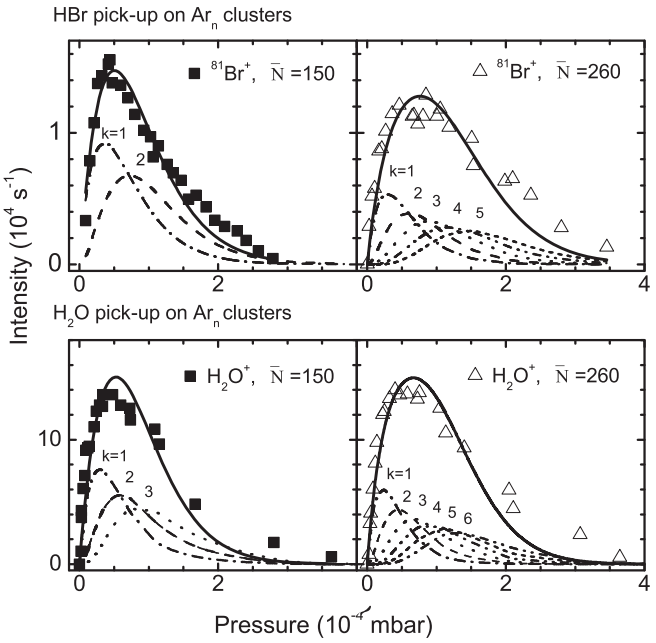

FIG. 5. Intensity of monomer fragment ion peaks in the mass spectra as a function of the pickup chamber pressure. The detected ions were Br^+ ($m/z = 81$ amu) and H_2O^+ ($m/z = 18$ amu) for HBr and H_2O pickup, respectively. The solid lines represent the fits to the data with a sum of Poisson distributions (see Eq. (12)).

H_2O^+ to monitor $k = 1$ pickup and $(H_2O)H^+$ for $k = 2$, and fit these dependencies with the corresponding Poisson statistics.

Finally for HBr pickup the necessity of a higher mass resolution (to resolve various fragments with ^{79}Br and ^{81}Br isotopes) limited the monitored mass range of our quadrupole below the mass of 150 amu. Due to this reason the HBr cluster ion peaks were not measured. However, an appreciable signal from $H^{81}BrH^+$ at $m/z = 83$ amu manifests the presence of $(HBr)_k$ clusters with $k \geq 2$. We have monitored ^{81}Br for the molecule $k = 1$ pickup and $H^{81}BrH^+$ peak for $k = 2$ capture. The intensity at 81 amu has been corrected for a contribution from $H^{79}BrH^+$. This could be done since the ^{81}Br:^{79}Br = 0.973 ratio is known and the $^{81}HBrH^+$ peak was measured.

The experimental data can be illustrated by the example in Fig. 4 which shows the H_2O^+ ion intensity dependence on the water pickup pressure. The solid line corresponds to the Poisson distribution fit to the data using Eq. (6) with $k = 1$ and σ_e as a fitting parameter. However, the obtained cross section $\sigma_e \approx 528$ Å^2 is significantly smaller than 848 Å^2 obtained for the same clusters from the velocity measurements. If the later value was used for Poisson fit with $k = 1$ (dashed line in Fig. 4), the experimental data could not be fitted adequately. Similar results were obtained for the other picked up molecules and the obtained cross sections are summarized in Table I. They will be further discussed in Sec. VI.

Figure 5 shows several examples of pickup data for HBr (top) and H_2O (bottom) molecules. Here the data are fitted by a sum of Poisson distributions with constant cross section σ_e (Eq. (6)) fixed to the value obtained from the velocity measurements. The fitting parameter was the number m of added $P_k(p)$, $k = 1, \ldots, m$. This is further discussed in Sec. VI.

V. MOLECULAR DYNAMICS AND MONTE CARLO SIMULATIONS

In order to support the experimental data we have performed molecular dynamics (MD) and Monte Carlo (MC) simulations of the pickup process. The simulations were performed in the coordinate system in which the cluster is initially at rest and the projectiles were shot at the cluster with the mean velocity corresponding to the experimental cluster beam velocity (490 ms^{-1}). The simulations were performed for the Ar_N cluster size $N = 150$ for three projectiles: Ar, HBr, and H_2O.

The Lennard-Jones (LJ) potential of the form

$$V_{LJ}(r) = 4\varepsilon \left(\left(\frac{\rho}{r}\right)^{12} - \left(\frac{\rho}{r}\right)^{6} \right) \qquad (8)$$

has been used for the description of Ar-Ar, HBr-Ar, and H_2O-Ar interactions. The parameters ε and ρ of the potential are listed in Table II. The parameters for Ar-Ar interaction have been obtained in Ref. 49 by fitting the correct pairwise potential of Aziz and Slaman.[56] It has been shown, that the LJ parameters usually used for simulation of liquids and solids cannot be used for simulations of cryogenic clusters.[49] Both HBr and H_2O were represented as united atom. The parameters for HBr-Ar potential were obtained in Ref. 48 by averaging the three body potential of Hutson[57] over all possible HBr orientations. The isotropic potential for H_2O-Ar has been successfully used to model argon-water ice collisions.[58,59] The parameters for H_2O-Ar potential were taken from Ref. 58. The use of isotropic potential is a relatively crude approximation; however, it has been applied previously for MD simulation of pickup of hydrogen halides on rare gas clusters and yielded good agreement with experiments.[47,48] As seen below, the present simulations agree very well with the experiment also for the H_2O-Ar_N system, which justifies the use of the isotropic potential also in this case. Because of the relative complexity of the CH_3OH molecule, the simulation of the

TABLE II. Lennard-Jones potential parameters used for molecular dynamics simulations.

	ρ (Å)	ε (K)
Ar-Ar	3.35	143.2
HBr-Ar	3.55	174
H_2O-Ar	3.0	174

methanol-Ar_N collisions is beyond the scope of the present mostly experimental paper.

We have used the Verlet's algorithm with a time step of 1 fs to integrate Newton's equation of motion. Simulation of one trajectory went as follows: The icosahedral structure of Ar_{150} cluster was assumed with coordinates taken from Cambridge cluster database.[60] The temperature of the cluster was assumed to be 32 K (Ref. 29) and the cluster was equilibrated for 10 ps. Then the cluster was randomly oriented and the projectile was shot at the cluster with a certain impact parameter. The impact velocity was sampled from the Maxwell-Boltzmann distribution of projectile gas at 300 K centered around 490 ms^{-1}. For each trajectory, the simulation lasted for 1 ns. After the simulation was finished, it was determined whether the projectile remained on the cluster, how many argon atoms were evaporated from the cluster, and the velocity of the cluster after the collision.

In order to calculate the pickup cross section, 2500 projectile trajectories were generated with random impact parameters and the cross section was evaluated from the ratio of sticking to nonsticking trajectories. This approach is illustrated in Fig. 6. The normally constant maximal impact parameter at which the collision is sticking has been diffused by the fact, that the projectiles have also transversal velocities sampled from the Maxwell-Boltzmann distribution. The pickup cross sections obtained from these simulations are listed in Table I.

In addition to the pickup cross section, the simulations addressed two questions that justify evaluation of the experimental data according to Eq. (5): (i) Are collisions with the gas in the pickup cell elastic or inelastic? (ii) Does the collision lead to an effective evaporation of cluster constituents? The bottom panel of Fig. 6 shows the histogram of simulated final cluster velocities for sticking and nonsticking collisions. The plot demonstrates that a considerable momentum transfer between the projectile and the cluster occurs only in the case of sticking collisions, i.e., in inelastic events. Also, the mean value of the final cluster beam velocity distribution is in excellent agreement with Eq. (3). No evaporation from the cluster was observed on the timescale of the simulation (1 ns).

We have addressed one more question using the simulations: If two HBr molecules are picked up on the Ar_{150} cluster, what is the probability that they coagulate, i.e., form the HBr dimer? The simulation was done as follows: the first HBr projectile was shot at the cluster with a random impact parameter (within the sticking range) and the system was simulated for 500 ps. Then the second HBr projectile was shot at this cluster with a random impact parameter and the system was simulated for 1 ns. The distance between the two HBr atoms

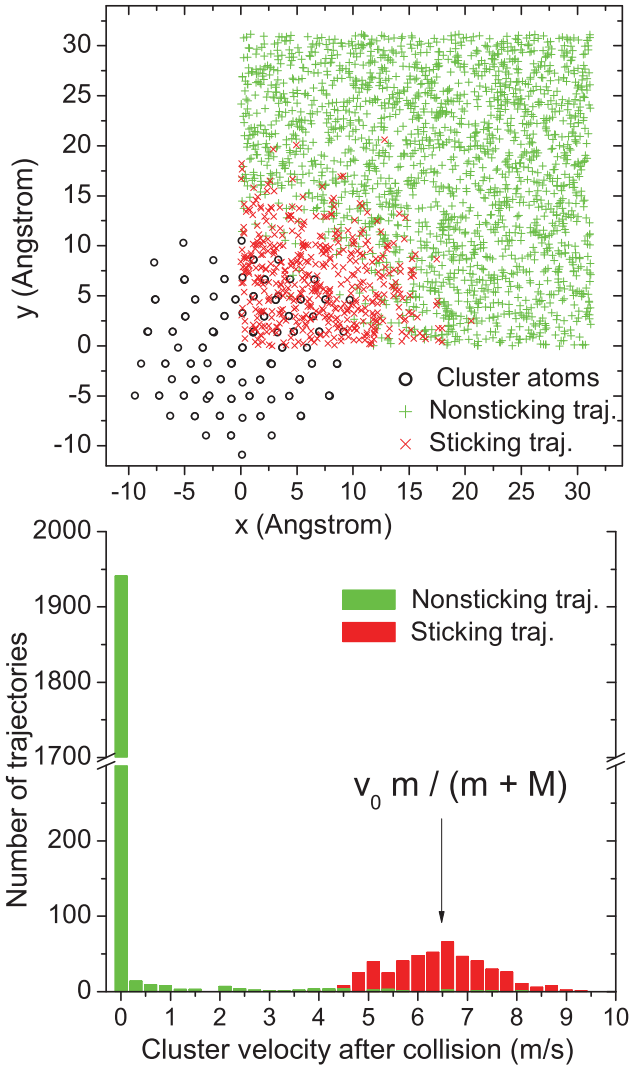

FIG. 6. Results of MD simulations for Ar_{150}-HBr collisions. Top: Map of sticking and nonsticking trajectories used to evaluate effective cross section. Bottom: Histogram for cluster velocities after the collisions. In the simulations the HBr projectiles were shot at the cluster initially in rest with the velocity corresponding to the experimental velocity of the cluster beam. The vertical arrow indicates the velocity shift according to Eq. (3) in excellent agreement with the simulations.

was monitored and if the average distance was less than 5 Å the coagulation was considered to occur (in all cases when the dimer was formed it did not dissociate till the end of the simulation). Total 2500 simulations were run and the coagulation occurred in 22.6% of cases. The mean time of dimer formation was 93 ps after the impact of the second projectile on the cluster.

The HBr-HBr interaction has been approximated by the isotropic hard-core Lennard-Jones (HCLJ) potential of Hurly,[61]

$$V_{HCLJ}(r) = 4\varepsilon\left(\left(\frac{\rho - 2a}{r - 2a}\right)^{12} - \left(\frac{\rho - 2a}{r - 2a}\right)^{6}\right) \qquad (9)$$

with the parameters $\varepsilon = 533.45$ K, $\rho = 3.44$ Å, and $a = 0.526$ Å. This potential approximates the HBr dimer by a diatomic-like molecule with isotropic interaction. We are

aware of the crudeness of such approximation – the present results do not properly describe the behaviour of two HBr molecules on Ar cluster. A proper interpretation of the simulation is that it describes the behaviour of two picked up atom-like objects that have the same binding energy as the HBr dimer. Nonetheless, results of such simulation – coagulation only in about 23% of cases – are helpful to understand the discrepancy in the experimental methods (see the discussion in Sec. VI A).

VI. DISCUSSION

A. Capture cross sections

The major point to be discussed here is the comparison of the pickup cross sections summarized in Table I. First, we focus on the effective cross sections σ_e evaluated from the velocity measurements which are in a good agreement with the simulated ones: in all cases the calculated cross sections exceed the measured ones by about 10% for HBr and H_2O and by 14% for Ar. The agreement between the velocity measurements and simulations suggests that the cross sections determined by this method are close to the real values.

It is interesting to note that σ_0 is consistent for all the molecules except methanol; i.e., $\sigma_0 \approx 570$ Å^2 for $\bar{N} = 150$ with all the values within 4%, and $\sigma_0 \approx 775$ Å^2 for $\bar{N} = 260$ with all the values within 10%. For methanol significantly larger σ_0 were obtained which could be caused by the fact that velocity correction factors corresponding to the hard sphere potential approximation is not valid for this large molecule with internal structure and many degrees of freedom. It should be also noted that the simulated cross sections were calculated in a way that mimics the experiment, thus they correspond to the effective cross section σ_e, i.e., the velocity correction factors F_{a0} are implicitly included. Both, in the experiment and simulations the cross sections are obtained on the assumption, that the projectile is a point-like particle, i.e., the size of the incoming molecule is neglected, or more precisely included in the obtained σ_e. This may add a small relative shift, especially for molecules like methanol.

We also compare the obtained cross sections to the simple geometrical cross sections. To determine the cluster mean size $\bar{N}$ by any of the two methods exploited here a certain analytical relationship between the cross section σ and N had to be assumed. Both Cuvellier *et al.*[36] and Macler and Bae,[3] assumed a geometrical pickup cross sections when introducing their methods for the mean cluster size determination, i.e.,

$$\sigma_g = \pi R_N^2, \quad R_N = \left(\frac{3a^3}{16\pi} N\right)^{1/3}, \tag{10}$$

where $a = 5.34$ Å is the lattice parameter of Ar clusters.[29] The geometrical cross sections corresponding to the present mean cluster sizes $\bar{N} = 150$ and 260 are $\sigma_g = 390$ Å^2 and 560 Å^2, respectively. Cuvellier *et al.*[36] used collision dynamics simulations to account for a more realistic attractive interaction of the molecule with the cluster and modified the geometrical cross section formula to

$$\sigma_{g0} = \pi(R_N + R_0)^2. \tag{11}$$

The value $R_0 = 3$ Å was determined by the simulations of Ar-Ar_{125} system. This yields the geometrical cross section $\sigma_{g0} = 620$ Å^2 and 840 Å^2 for the present mean cluster sizes $\bar{N} = 150$ and 260, respectively.

Clearly the simple hard sphere cross sections σ_g (Eq. (10)) are strongly underestimated. Adopting the approach of Cuvellier *et al.*[36] we can modify σ_g by the contribution R_0 due to the interaction between the cluster and the projectile to σ_{g0} (Eq. (11)). Thus from comparison of the simulated cross sections with σ_g, the parameter R_0 can be evaluated (Table I). Note, that the comparison was made with the calculated σ_e value which implicitly includes also the velocity dependence (F_{a0}) thus R_0 is in principle velocity dependent. Since this parameter is due to the interaction between the species, it should correlate with the potential parameters in Table II. It is interesting to note that R_0 increases with the decreasing parameter ρ of LJ potential.

The most striking observation is the significantly smaller cross sections evaluated from the Poisson distributions. The Poisson statistics is frequently used to determine the number k of particles picked up by the cluster.[2,7,16,19] Generally the good quality of the Poisson distribution fit to the experimental data is regarded as the justification for using such analysis to obtain k, $\bar{N}$, or σ values. The present measurements show that, although high quality fits could be obtained, the evaluated cross sections still differ significantly from the real values. An indication that the σ_e values are wrong is the fact that they are larger for the smaller clusters in all cases.

Also the second order $k = 2$ Poisson distributions were fitted to the corresponding signals for all three studied molecules, e.g., at masses $m/z = 19$ amu [H_2OH^+], 33 amu [$(CH_3OH)H^+$], and 83 amu [$HBr^{81}H^+$]. However, even smaller cross sections were obtained from these fits than from the $k = 1$ fragments. The quality of these fits was somewhat worse with evident broadening in the high pressure region.

Below several factors are addressed that complicate the emergence of the Poisson statistics and could explain why the analysis yields the lower cross sections. We argue that some of these factors (i.e., non-sticking collisions, evaporation, and scattering from the beam) do not contribute to present discrepancy, while other factors (i.e., coagulation and fragmentation upon ionization) can contribute.

The first possible reason for the discrepancy could be the *non-sticking* collisions. If the sticking coefficient of a molecule is $s < 1$, only a fraction of the total number of collisions will actually result in the capture of the molecule on the cluster. On the other hand, the cluster can be slowed down even in an inelastic collision, which does not result in complete momentum transfer and the sticking of the molecule to the cluster. However, as is demonstrated in Fig. 6, the simulations suggest that the measured velocity decrease is caused almost exclusively by the sticking collisions, and thus the cross sections obtained by both methods should be the same.

Further effect can be an *evaporation* of the Ar cluster atoms due to the energy transfer in the sticking collision. This effect would lower the cross section for each subsequent pickup event, since $\sigma \propto \bar{N}^{2/3}$. The molecular

dynamics simulations did not show any evaporation within 1 ns after the pickup. The large clusters are efficient thermal baths for energy dissipation and a significant evaporation on longer timescale is not expected. The following energy arguments can be also used. For the binding energy of a single Ar atom to the Ar_N cluster $N = 150$ a model calculation[62] as well as our estimate based on the LJ potential yield ~80 meV. The binding energy of an HBr molecule to the cluster can be estimated from the Ar-Ar_N binding energy and the comparison of the LJ potentials for Ar-Ar and HBr-Ar interactions (Table II), i.e., the HBr-Ar_N energy would correspond to ~100 meV. Upon the pickup of a single HBr molecule this binding energy plus the heat due to collision inelasticity (~100 meV) are transferred to the cluster, i.e., total about 200 meV which would be sufficient to evaporate only two Ar atoms. This effect could not explain the observed cross section decrease.

The *scattering* of clusters on molecules in the pickup cell can deflect the smaller clusters out of the beam to a greater extent than the large ones, and thus shift the mean cluster size to a larger value. This effect could make the observed capture cross section larger which, however, is not the case.[63] Additionally, this effect would influence both experimental methods simultaneously.

One explanation of the observed difference concerns the *coagulation* of the embedded molecules. It was discussed in detail for He clusters,[2–4] however, the present case of solid-like argon clusters might differ significantly from the superfluid helium nanodroplets. The coagulation on Ar clusters will be controlled by a competition between the polarization forces attracting the molecules towards each other and the forces binding the molecules to the cluster and hindering their diffusion on the surface. This issue has been also addressed with our MD simulations (Sec. V) for two HBr-like objects picked up by the cluster. The coagulation (i.e, the formation of HBr dimer on the cluster surface) occurred only in 22.6% out of 2500 simulations. If the picked up molecules do not coagulate, even the pickup of $k \geq 2$ molecules will contribute to the signal assigned to the monomer. This signal is, however, fitted with $k = 1$ distribution $P_k(p)$. Thus the ion signal dependence corresponding to the monomer will be a composition of several independent events where $k = 1,2,...$ molecules are picked up by the cluster. Figure 5 shows the experimental data fitted with a sum of Poisson distributions,

$$P(p) = A_0 \sum_{k=1}^{m} P_k(p). \tag{12}$$

In the nonlinear least-squares fit procedure the number m of P_k distributions (Eq. (6)) was varied while the parameter σ was fixed to the value obtained from the velocity experiment. From these fits it would follow that Ar clusters of size $\bar{N} = 150$ can accommodate up to $m = 3$ water molecules without coagulation. The distribution for larger clusters is even broader with up to $m = 6$ water molecules. This would imply very poor migration of the guest molecule on the Ar cluster.

Yet another important issue is the *fragmentation* of the host molecule or cluster upon the ionization. The assumption that we measure the Poisson distribution for the pickup of k molecules X can be only valid if we detect a fragment which corresponds exclusively to the ionization of X_k species, i.e., for P_1 distribution we have to choose the fragment which corresponds exclusively to the monomer ionization and not to the ionization of an $X_{k\geq 2}$ cluster. However, the fragmentation dynamics can be more complicated and affected by the Ar cluster. For example, the accepted fast proton transfer reaction as a main fragmentation channel for the hydrogen bonded clusters after ionization can be quenched by the cluster environment as observed for the methanol clusters on larger Ar clusters.[18] Thus, even if the molecules coagulate and form the dimer, upon ionization the dimer fragment can contribute to P_1 distribution and the fit will yield erroneous result for the cross section.

In summary, due to incomplete coagulation and ionization fragmentation dynamics the pickup of $k \geq 2$ molecules can still contribute to the measured intensity of the fragment assigned to the pickup of a single molecule. The dependence of the fragment intensity on the pickup pressure will thus extend to higher pressures which will result in smaller fitted σ_e if the fit with a single Poisson ($k = 1$) distribution is used. It ought to be mentioned that in some cases dependencies with clearly enhanced intensity at higher pressures have been measured. Thus the pickup cross section evaluated from the Poisson distribution fit will be smaller than the real cross section.

B. Implications for cluster size determination

Two methods for the mean cluster size determination based on the pickup process were examined in our study.[36,37] Since the cluster mean size $\bar{N}$ and the pickup cross section σ cannot be determined independently by these methods, both methods assumed a certain analytical relationship between these two quantities which was the geometrical cross section of a hard sphere. Our original motivation for these measurements was that by combining Eqs. (5) and (6), both quantities σ and $\bar{N}$ could be determined by simultaneous measurements of velocity and Poisson distributions. This would present a new method for determining the mean cluster size in a beam without the geometrical cross section assumption.

However, as seen above, in the course of our pickup measurements we have discovered that the two methods actually provide inconsistent results. The reason is that in the Poisson distribution measurements, incomplete coagulation of molecules on the cluster surface and their fragmentation patterns complicate the fitting procedure. Since these processes are not always obvious, it has to be cautiously examined which species are actually detected in the Poisson distribution measurements, if the cluster size or cross section are to be determined from such data. In other words, if the mean cluster size or cluster cross section is based solely on the Poisson distribution $P_k(p)$ measurement of a certain fragment after the pickup process, the result can be wrong, unless the measured fragment ion is assigned unambiguously to the

pickup of k molecules and any contribution from pickup of more than k molecules is excluded.

VII. CONCLUSIONS

We report here the capture cross sections σ_e for pickup of several gas molecules (HBr, H_2O, CH_3OH) and Ar atoms on Ar_N clusters of the mean sizes $\bar{N} \approx 150$ and 260. Two different methods proposed in the literature[36,37] were employed in the present measurements and σ_e was evaluated from

1. the decrease in the cluster beam velocity due to the momentum transfer of the picked up molecules;
2. the Poisson distribution fit of a selected cluster fragment ion intensity dependence on the pickup pressure.

In addition, the pickup cross sections were calculated with molecular dynamics and Monte Carlo simulations. The simulations support the results of the velocity measurements. On the other hand, the Poisson distributions yield significantly smaller cross sections, which are also inconsistent with the dependence on the cluster size. The reasons for the inconsistency of the results based on the Poisson distributions are discussed in terms of (i) an incomplete coagulation of guest molecules on the argon clusters when $k \geq 2$ molecules are picked up, and (ii) the fragmentation pattern of the embedded molecules and their clusters upon ionization on the Ar cluster.

The general message from this paper is that the Poisson distribution method has to be cautiously examined, if conclusions should be drawn about the cluster mean size $\bar{N}$, or the cross section σ, or the number k of picked up molecules.

It is also important to note that both the velocity measurements as well as the MC simulations show that the simple geometrical cross sections are significantly smaller than the real values and therefore not a good approximation for the cluster pickup cross section.

ACKNOWLEDGMENTS

This work has been supported by the Grant Agency of the Czech Republic Project Nos. 203/09/0422 and P208/11/0161, and the Academy of Sciences of the Czech Republic Project No. KJB400400902. J. Fedor acknowledges the support of the Grant No. 235414 "IPhoN" within FP7-MC-IEF. We gratefully acknowledge discussing our results with Udo Buck.

[1] T. E. Gough, M. Mengel, P. A. Rowntree, and G. Scoles, J. Chem. Phys. **83**, 4958 (1985).
[2] M. Lewerenz, B. Schilling, and J. P. Toennies, J. Chem. Phys. **102**, 8191 (1995).
[3] M. Macler and Y. K. Bae, J. Chem. Phys. **106**, 5785 (1997).
[4] M. Lewerenz, B. Schilling, and J. P. Toennies, J. Chem. Phys. **106**, 5787 (1997).
[5] M. Hartmann, R. E. Miller, J. P. Toennies, and A. F. Vilesov, Phys. Rev. Lett. **75**, 1566 (1995).
[6] S. Grebenev, J. P. Toennies, and A. F. Vilesov, Science **279**, 2083 (1998).
[7] M. Behrens, R. Fröchtenicht, M. Hartmann, J. G. Siebers, and U. Buck, J. Chem. Phys. **111**, 2436 (1999).
[8] G. Scoles and K. K. Lahmann, Science **287**, 2429 (2000).
[9] J. P. Toennies and A. F. Vilesov, Angew. Chem., Int. Ed. **43**, 2622 (2004).
[10] M. Y. Choi, G. E. Douberly, T. M. Falconer, W. K. Lewis, C. M. Lindsay, J. M. Merritt, P. L. Stiles, and R. E. Miller, Int. Rev. Phys. Chem. **25**, 15 (2006).
[11] E. Lugovoj, J. P. Toennies, and A. F. Vilesov, J. Chem. Phys. **112**, 8217 (2000).
[12] M. Fárník and J. P. Toennies, J. Chem. Phys. **122**, 014307 (2005).
[13] J. M. Merritt, S. Rudić, and R. E. Miller, J. Chem. Phys. **124**, 084301 (2006).
[14] S. Denifl, F. Zappa, I. Mähr, F. Ferreira da Silva, A. Aleem, A. Mauracher, M. Probst, J. Urban, P. Mach, A. Bacher, O. Echt, T. D. Märk, and P. Scheier, Angew. Chem., Int. Ed. **121**, 9102 (2009).
[15] A. Gutberlet, G. Schwaab, O. Birer, M. Masia, A. Kaczmarek, H. Forbert, M. Havenith, and D. Marx, Science **324**, 1545 (2009).
[16] J. M. Mestdagh, M. A. Gaveau, C. Gée, O. Sublemontier, and J. P. Visticot, Int. Rev. Phys. Chem. **16**, 215 (1997).
[17] M.-A. Gaveau, E. Glogauen, P.-R. Fournier, and J.-M. Mestdagh, J. Phys. Chem. A **109**, 9494 (2005).
[18] M. Ehbrecht, M. Stemmler, and F. Huisken, Int. J. Mass. Spectrom. **123**, R1 (1993).
[19] U. Buck, J. Phys. Chem. A **106**, 10049 (2002).
[20] V. Poterya, M. Fárník, P. Slavíček, U. Buck, and V. V. Kresin, J. Chem. Phys. **126**, 071101 (2007).
[21] V. Poterya, O. Votava, M. Fárník, M. Ončák, P. Slavíček, U. Buck, and B. Friedrich, J. Chem. Phys. **128**, 104313 (2008).
[22] V. Poterya, J. Fedor, A. Pysanenko, O. Tkáč, J. Lengyel, M. Ončák, P. Slavíček, and M. Fárník, Phys. Chem. Chem. Phys. **13**, 2250 (2011).
[23] C. Nitsch, C. P. Schulz, A. Gerber, W. Zimmermann-Edling, and I. V. Hertel, Z. Phys. D: At., Mol. Clusters **22**, 651 (1992).
[24] M. Ahmed, C. J. Apps, C. Hughes, N. E. Watt, and J. C. Whitehead, J. Phys. Chem. A **101**, 1250 (1997).
[25] H. Haberland, *Clusters of Atoms and Molecules* (Springer, Berlin, 1994).
[26] U. Buck and H. Meyer, Phys. Rev. Lett. **52**, 109 (1984).
[27] U. Buck and H. Meyer, J. Chem. Phys. **84**, 4854 (1986).
[28] T. D. Märk, in *Linking the Gaseous and Condensed Phases of Matter*, edited by L. G. Christopherou (Plenum, New York, 1994), p. 155.
[29] J. Farges, M. F. de Feraudy, B. Raoult, and G. Torchet, Sur. Sci. **106**, 95 (1981).
[30] J. Farges, M. F. de Feraudy, B. Raoult, and G. Torchet, J. Chem. Phys. **78**, 5067 (1983).
[31] G. Torchet, P. Schwartz, J. Farges, M. F. de Feraudy, and B. Raoult, J. Chem. Phys. **79**, 6196 (1983).
[32] J. Farges, M. F. de Feraudy, B. Raoult, and G. Torchet, J. Chem. Phys. **84**, 3491 (1986).
[33] A. D. Martino, M. Benslimane, M. Châtelet, C. Crozes, F. Padère, and H. Vach, Z. Phys. D: At., Mol. Clusters **27**, 185 (1993).
[34] C. Bobbert, S. Schütte, C. Steinbach, and U. Buck, Eur. Phys. J. D **19**, 183 (2002).
[35] U. Buck and R. Krohne, J. Chem. Phys. **105**, 5408 (1996).
[36] J. Cuvellier, P. Meynadier, P. de Pujo, O. Sublemontier, J.-P. Visticot, J. Berlande, A. Lallement, and J.-M. Mestdagh, Z. Phys. D: At., Mol. Clusters **21**, 265 (1991).
[37] M. Macler and Y. K. Bae, J. Phys. Chem. A **101**, 145 (1997).
[38] O. F. Hagena, Surf. Sci. **106**, 101 (1981).
[39] O. F. Hagena, Z. Phys. D: At., Mol. Clusters **4**, 291 (1987).
[40] O. F. Hagena, Rev. Sci. Instrum. **63**, 2374 (1992).
[41] R. Baumfalk, N. H. Nahler, U. Buck, M. Y. Niv, and R. B. Gerber, J. Chem. Phys. **113**, 329 (2000).
[42] R. Baumfalk, U. Buck, C. Frischkorn, S. R. Gandhi, and C. Lauenstein, Ber. Bunsenges. Phys. Chem. **101**, 606 (1997).
[43] M. Fárník, *Molecular Dynamics in Free Clusters and Nanoparticles Studied in Molecular Beams* (ICT Prague Press, Institute of Chemical Technology Prague, 2011).
[44] The experiments were also performed with a small pickup cell of $L = 5$ cm length placed in the next vacuum chamber. Since the capture probability is proportional to L and the pickup gas pressure p, using the chamber with longer pickup path allowed to lower the pressure p resulting in a more precise pressure control and consequently better characterization of the pickup process. The results using the two different chambers were consistent within the experimental error.
[45] D. J. Auerbach, in *Atomic and Molecular Beam Methods*, edited by G. Scoles (Oxford University Press, New York, 1988), Vol. I, p. 362.
[46] H. Pauly, *Atom, Molecule and Cluster Beams* (Springer, Berlin, 2000).
[47] M. Fárník, N. H. Nahler, U. Buck, P. Slavíček, and P. Jungwirth, Chem. Phys. **315**, 161 (2005).
[48] N. H. Nahler, R. Baumfalk, U. Buck, H. Vach, P. Slavíček, and P. Jungwirth, Phys. Chem. Chem. Phys. **5**, 3394 (2003).

[49]P. Slavíček, P. Jungwirth, M. Lewerenz, N. H. Nahler, M. Fárník, and U. Buck, J. Chem. Phys. **120**, 4498 (2004).
[50]K. Berling, R. Belbing, K. Kramer, H. Pauly, C. Schlier, and P. Toschek, Z. Phys. **166**, 406 (1962).
[51]N. C. Lang, H. V. Lilenfeld, and J. L. Kinsey, J. Chem. Phys. **55**, 3114 (1971).
[52]U. Nagashima, H. Shinohara, N. Nishi, and H. Tanaka, J. Chem. Phys. **84**, 209 (1986).
[53]S. Morgan and A. W. Castleman, J. Phys. Chem. **93**, 4544 (1989).
[54]F. Huisken and M. Stemmler, Z. Phys. D: At., Mol. Clusters **24**, 277 (1992).
[55]U. Buck and M. Winter, Z. Phys. D: At., Mol. Clusters **31**, 291 (1994).
[56]R. A. Aziz and M. J. Slaman, Mol. Phys. **58**, 679 (1986).
[57]J. M. Hutson, J. Chem. Phys. **91**, 4455 (1989).
[58]K. Bolton, M. Svanberg, and J. B. C. Pettersson, J. Chem. Phys. **110**, 5380 (1999).
[59]P. U. Andersson, M. B. Någård, K. Bolton, M. Svanberg, and J. B. C. Pettersson, J. Phys. Chem. A **104**, 2681 (2000).
[60]D. J. Wales, J. P.K. Doye, A. Dullweber, M. P. Hodges, F. Y. Naumkin, F. Calvo, J. Hernández-Rojas, and T. F. Middleton, *The Cambridge Cluster Database*, available from http://www-wales.ch.cam.ac.uk/CCD.html.
[61]J. J. Hurly, Int. J. Thermophys. **21**, 805 (2000).
[62]K. Hansen and E. E.B. Cambell, Int. J. Mass. Spectrom. **233**, 215 (2004).
[63]We attempted to correct the data for the beam attenuation by using an exponential fit to observed decrease of the total pressure in the detector chamber. This results in somewhat larger evaluated cross sections, yet still not in agreement with the velocity measurements. Since only the small clusters can be deflected enough to escape the detection, the estimated error of the obtained cross sections due to this effect could be $\lesssim$10%.